

Control-Oriented Modeling of Fluid Networks: A Time-Delay Approach

David Novella-Rodriguez, Emmanuel Witrant and Olivier Sename

Abstract Fluid networks are characterized by complex interconnected flows, involving high order nonlinear dynamics and transport phenomena. Classical lumped models typically capture the interconnections and nonlinear effects but ignore the transport phenomena, which may strongly affect the transient response. To control such flows with regulators of reduced complexity, we improve a classical lumped model (obtained by combining Kirchhoff's laws and graph theory) by introducing the effect of advection as a time delay. The model is based on the isothermal Euler equations to describe the dynamics of the fluid through the pipe. The resulting hyperbolic system of partial differential equations (PDEs) is diagonalized using Riemann invariants to find a solution in terms of delayed equations, obtained analytically using the method of the characteristics. Conservation principles are applied at the nodes of the network to describe the dynamics as a set of (possibly non linear) delay differential equations. Both linearized and nonlinear Euler equations are considered.

1 Introduction

Modeling and control of fluid flow networks has been a challenging topic during the last decades. This research is motivated by engineering applications such as mine ventilation systems [17, 28], gas pipelines [2, 13], water channels [7, 21], traffic flow dynamics [27], cryogenic distribution lines [3], etc.

David Novella-Rodriguez
IPN, ESIME Culhuacan, Santa Ana 1000, C.P. 44300, México, e-mail: dnovellar@gmail.com

Emmanuel Witrant
Université de Grenoble, GIPSA-lab, Grenoble, France, e-mail: emmanuel.witrant@ujf-grenoble.fr

Olivier Sename
Université de Grenoble, GIPSA-lab, Grenoble, France, e-mail: olivier.sename@gipsa-lab.grenoble-inp.fr

For example, considering mining ventilation engineering, the first approaches used a steady-state description of the pipe network and models were built using the Hardy Cross method [8]. With this method, the airflow in mine ventilation circuits is determined algebraically by combining graph theory and classical Kirchhoff's laws to model the interconnection nodes [15]. In more recent approaches, a lumped parameter model for mine ventilation networks has been represented in terms of nonlinear ordinary differential equations [22, 17], with an extension to periodically forced networks in [19]. The model proposed in these works is based on Kirchhoff's voltage and current laws, combined with the fluid dynamical equations of individual branches. The branches are modeled by considering the incompressible Navier-Stokes equations as an electric equivalent RL circuit model with a nonlinear resistance. More precisely, the pressure drop over a branch is approximated to be proportional to the square of the air flow rate and to the air flow acceleration.

On the other hand, partial differential equations are often used to model fluid flows as hyperbolic conservation laws. For example, the Saint-Venant equations are used to approximate 2-D shallow water phenomena with a 1-D PDE model [10]. Such models have been extensively used to control open channel networks [7, 20, 21, 9, 5]. Another example is provided in mine ventilation networks [28], where Euler equations are used to describe the gas flow dynamics in pipelines [2, 14, 13, 11]. In a different field, a first order PDE has been proposed to describe the traffic flow density on an homogeneous road, obtaining the Lighthill Whitham Richards model [27]. However, such detailed dynamic models are typically complex and often incompatible with real-time control objectives. To reduce the computational load, a 0-D approximation of the 1-D transport (with advection and sink) as a time-delay system has been proposed in [29, 30] and shown to be efficient as a reference model for feedback control of the large advective flows appearing in the mining ventilation problem. A similar approach was used in [4] to model the temperature in an SI engine exhaust catalyst. Nevertheless, such approximations did not take into account the occurrence of interconnected flows or the simultaneous transport of multiple variables.

The aim of this work is to present a time-delay model for fluid flow networks, leading to a classical state-space representation with delays to take into account the transport phenomena in the pipes of the network. Describing the flow in the branches of the network as isothermal Euler equations, we consider the transport of both density and momentum. The hyperbolic characteristics of the system of PDEs is used to find a solution described by delayed equations. Applying conservation laws in the nodes of the network, we finally obtain a delay differential equation describing the fluid dynamics of the complete system.

This chapter is organized as follows. Section 2 presents the physical equations that model the flow inside the pipelines. A time-delay model, found by the method of characteristics, describes the isothermal Euler equations in terms of delayed equations in Section 3. Both linear and nonlinear approximations are taken into account. The conservation principles are introduced at the nodes in Section 4, providing a state-space description in terms of delay differential equations from which we ob-

tain the dynamics of the network. Numerical simulations of the time delay system are presented in Section 5.

2 Isothermal Euler Equations

A classical model for gas flow in pipe networks is provided by isothermal Euler equations [14, 13]. For such equations the temperature is constant and the pressure is given by the following state equation (e.g. for perfect gases):

$$P = \frac{ZRT}{M_g} \rho, \quad (1)$$

where Z is the natural gas compressibility factor, R the universal gas constant, T the absolute gas temperature, M_g the gas molecular weight, and $P(x,t)$ and $\rho(x,t)$ are the pressure and density of the gas, respectively. We consider a mono-dimensional description of the flow in terms of the space variable x . To simplify the notation, we define the speed of sound constant $a^2 = ZRT/M_g$ and the isothermal Euler equations are:

$$\frac{\partial \rho}{\partial t} + \frac{\partial q}{\partial x} = 0, \quad (2)$$

$$\frac{\partial q}{\partial t} + \frac{\partial}{\partial x} \left(\frac{q^2}{\rho} + a^2 \rho \right) = -f_g \frac{q |q|}{2D\rho}, \quad (3)$$

where $q(x,t)$ is the momentum, f_g is the friction factor, and D is the diameter of the pipe. The first equation states the conservation of mass and the second equation is the momentum equation.

The flux of the Euler equations is thus defined as [26]:

$$F = \begin{pmatrix} q \\ \frac{q^2}{\rho} + a^2 \rho \end{pmatrix},$$

and its Jacobian is

$$A(\rho, q) = \begin{pmatrix} 0 & 1 \\ a^2 - \frac{q^2}{\rho^2} & 2\frac{q}{\rho} \end{pmatrix}. \quad (4)$$

The eigenvalues of the Jacobian matrix $A(\rho, q)$, namely the characteristic velocities, are

$$\lambda_{1,2} = \frac{q}{\rho} \pm a. \quad (5)$$

The system of isothermal Euler equations (2) and (3) can be diagonalized using the Riemann invariants, some quantities that have the interesting property of remaining constant along special trajectories called the characteristic curves. This invariance property is crucial in the control design. The Riemann invariants are de-

finied by the change of coordinates [14]:

$$\xi_{1,2}(\rho, q) = -\frac{q}{\rho} \mp a \ln(\rho), \quad (6)$$

and we assume that the characteristic velocities (5) satisfy $\lambda_2 < 0 < \lambda_1$ (subsonic case), which characterizes the system as a strictly hyperbolic PDE. We can also express the physical variables ρ and q in terms of the Riemann coordinates as follows:

$$\rho = \exp\left(\frac{\xi_2 - \xi_1}{2a}\right), \quad (7)$$

$$q = -\frac{\xi_1 + \xi_2}{2} \exp\left(\frac{\xi_2 - \xi_1}{2a}\right). \quad (8)$$

With the new coordinates (ξ_1, ξ_2) , the system (2)-(3) can be written in the following diagonal form:

$$\frac{\partial \Xi(x, t)}{\partial t} + \Lambda(\Xi) \frac{\partial \Xi(x, t)}{\partial x} = S(\Xi), \quad (9)$$

where $\Xi(x, t) \doteq [\xi_1 \ \xi_2]^T$, and

$$\Lambda(\Xi) = \begin{bmatrix} -\frac{\xi_1 + \xi_2}{2} + a & 0 \\ 0 & -\frac{\xi_1 + \xi_2}{2} - a \end{bmatrix}. \quad (10)$$

The source term is then defined by:

$$S(\Xi) = -\frac{fg}{8D} (\xi_1 + \xi_2) |\xi_1 + \xi_2| \begin{pmatrix} 1 \\ 1 \end{pmatrix}, \quad (11)$$

The initial and boundary conditions are given by

$$\xi_1(x, 0) = \phi_1(x), \quad (12)$$

$$\xi_2(x, 0) = \phi_2(x), \quad (13)$$

$$\xi_1(0, t) = u_1(t), \quad (14)$$

$$\xi_2(L, t) = u_2(t). \quad (15)$$

3 Time Delay Model

There is a connection between the boundary problems for one-dimensional hyperbolic partial differential equations, namely with a single space coordinate accounting for wave propagation, and functional equations. These functional equations may be defined as difference, delay-differential or even integral or integro-differential

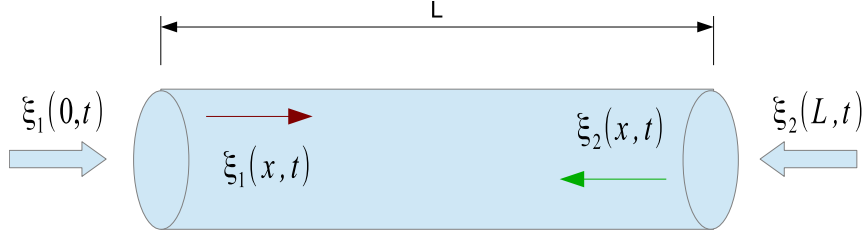


Fig. 1 Wave Propagation

equations [23], [24]. Conservation laws are typically described by nonlinear hyperbolic PDE belonging to the “lossless” (or conservative) class.

This connection between two different mathematical objects, the hyperbolic PDEs and the functional equations, has been considered in many studies. For instance, in [6] delayed differential equations are derived to describe the propagation phenomena in power lines. On the other hand, in [25] neutral differential models are developed for different hyperbolic conservation laws (namely, circulating fuel in nuclear reactors, control of an overhead crane with flexible cable, etc.). From a different perspective, [30] proposes a distributed time-delay system to describe large convective flows modeled by linear time-varying partial differential equations (e.g. Euler or Navier-Stokes equations). In the recent work [18] the equivalence between systems described by a single first-order hyperbolic partial differential equation and systems described by integral delay equations is stated.

Consider the flow propagation in a pipe described in Fig. 1, with boundary conditions $\xi_1(0,t)$ and $\xi_2(L,t)$. In this section, we develop a model based on the nonlinear hyperbolic system described by isothermal Euler equations expressed in terms of the Riemann invariants:

$$\frac{\partial}{\partial t} \begin{bmatrix} \xi_1 \\ \xi_2 \end{bmatrix} + \begin{bmatrix} \lambda_1 & 0 \\ 0 & \lambda_2 \end{bmatrix} \frac{\partial}{\partial x} \begin{bmatrix} \xi_1 \\ \xi_2 \end{bmatrix} = \begin{bmatrix} -\alpha(\xi_1 + \bar{\xi}_2)^2 \\ -\alpha(\bar{\xi}_1 + \xi_2)^2 \end{bmatrix}, \quad (16)$$

Where λ_1 and λ_2 are the characteristic velocities of the hyperbolic system. We averaged the quantities ξ_1 and ξ_2 as $\bar{\xi}_1$ and $\bar{\xi}_2$ (i.e., average equilibrium values in the pipe volume), respectively, to avoid the internal coupling between the two waves and allow finding a solution in terms of a time-delay equation. Note that this approximation is not strictly necessary, as an equivalent functional equation with a delayed kernel can be derived for the coupled case, but we adopt it here to simplify the derivations and focus on the major transport effects. We first consider the linearized case and then investigate the impact of the squared term.

3.1 Linear Approximation

Our approach extends the results in [30] to the multiple variable case and is based on the method of characteristics. This method makes it possible to reduce a partial

differential equation to a system of ordinary differential equations; see for instance [12] for more details. Here, this method provides the functional equations related to the isothermal Euler equations in Riemann coordinates.

To apply the method of characteristics to the isothermal Euler equations, a linear approximation of the source term (11) is first adopted. From (6) and assuming a mono-directional flow, namely $q > 0$ (and $\rho > 0$ by definition), we have:

$$|\xi_1 + \xi_2| = -(\xi_1 + \xi_2). \quad (17)$$

Taking into account the averaged terms in (16) and from the assumption (17), it is possible to obtain a linearization around the equilibrium point $(\bar{\xi}_1, \bar{\xi}_2)$ as:

$$S(\Xi) \simeq 2\alpha \begin{bmatrix} (\bar{\xi}_1 + \bar{\xi}_2) & 0 \\ 0 & (\bar{\xi}_1 + \bar{\xi}_2) \end{bmatrix} \begin{bmatrix} \xi_1 \\ \xi_2 \end{bmatrix}. \quad (18)$$

where $\alpha = \frac{f_g}{8D}$. We thus obtain the following decoupled PDE system:

$$\frac{\partial}{\partial t} \begin{bmatrix} \xi_1 \\ \xi_2 \end{bmatrix} + \begin{bmatrix} \lambda_1 & 0 \\ 0 & \lambda_2 \end{bmatrix} \frac{\partial}{\partial x} \begin{bmatrix} \xi_1 \\ \xi_2 \end{bmatrix} = 2\alpha \begin{bmatrix} (\bar{\xi}_1 + \bar{\xi}_2) & 0 \\ 0 & (\bar{\xi}_1 + \bar{\xi}_2) \end{bmatrix} \begin{bmatrix} \xi_1 \\ \xi_2 \end{bmatrix}. \quad (19)$$

With the previous assumptions and taking into account the PDE system (19) the solution for each wave can be found by the *method of characteristics* [12, 30]. First, the propagation wave ξ_1 satisfies:

$$\frac{\partial \xi_1}{\partial t} + \lambda_1 \frac{\partial \xi_1}{\partial x} = 2\alpha(\bar{\xi}_1 + \bar{\xi}_2)\xi_1, \quad (20)$$

with the initial and boundary conditions (12) and (14), respectively. We can construct a characteristic curve s_1 emanating from $(0, t_0, u_1(t_0))$ and look for a solution to the following characteristic equations:

$$\frac{dt}{ds_1} = 1, \quad (21)$$

$$\frac{dx}{ds_1} = \lambda_1, \quad (22)$$

$$\frac{dz_1}{ds_1} = 2\alpha(\bar{\xi}_1 + \bar{\xi}_2)z_1(s_1), \quad (23)$$

which satisfies the initial conditions $t(0) = t_0$, $x(0) = 0$, and $z_1(0) = u_1(t_0)$. A simple integration of the ODE system leads to

$$t = s_1 + t_0, \quad (24)$$

$$x = \lambda_1 s_1, \quad (25)$$

$$z_1 = u_1(t_0)e^{2\alpha(\bar{\xi}_1 + \bar{\xi}_2)s_1}. \quad (26)$$

After an appropriate change of variables, we obtain the following solution:

$$\xi_1(x, t) = \xi_1 \left(0, t - \frac{x}{\lambda_1} \right) e^{2\alpha(\bar{\xi}_1 + \bar{\xi}_2) \frac{x}{\lambda_1}}. \quad (27a)$$

Similarly, applying the method of characteristics to the second propagation wave leads to:

$$\xi_2(x, t) = \xi_2 \left(L, t - \frac{(L-x)}{\lambda_2} \right) e^{2\alpha(\bar{\xi}_1 + \bar{\xi}_2) \frac{(L-x)}{\lambda_2}}. \quad (27b)$$

Note that λ_1 and λ_2 are of opposite sign and ξ_1 and ξ_2 are propagated in opposite directions. Note also that these results still holds for time-varying characteristic velocities, which would result in time-varying time-delays.

From (27a) and (27b) at their boundaries, it is thus possible to describe the flow transport by the following difference equations:

$$\xi_1(L, t) = \xi_1(0, t - h_1) e^{2\alpha(\bar{\xi}_1 + \bar{\xi}_2)h_1}, \quad (28a)$$

$$\xi_2(0, t) = \xi_2(L, t - h_2) e^{2\alpha(\bar{\xi}_1 + \bar{\xi}_2)h_2}, \quad (28b)$$

where $h_i = L/\lambda_i$.

3.2 Nonlinear Approximation

Calculating the characteristics of (16) without linearizing, we obtain a solution for the PDE hyperbolic system (16) using the following ODE system:

$$\frac{dt}{ds_1} = 1, \quad (29)$$

$$\frac{dx}{ds_1} = \lambda_1, \quad (30)$$

$$\frac{dz_1}{ds_1} = -\alpha(z_1 + \bar{\xi}_2)^2, \quad (31)$$

which satisfies the initial conditions

$$t(0) = t_0, \quad x(0) = 0, \quad z_1(0) = u_1(t_0). \quad (32)$$

Integrating this ODE system implies that:

$$t = s_1 + t_0, \quad (33)$$

$$x = \lambda_1 s_1, \quad (34)$$

$$z_1(s_1) = -\bar{\xi}_2 + \frac{z_1(0) + \bar{\xi}_2}{\alpha s_1 (z_1(0) + \bar{\xi}_2) + 1}. \quad (35)$$

Finally substituting the initial conditions (32) in (35) leads to:

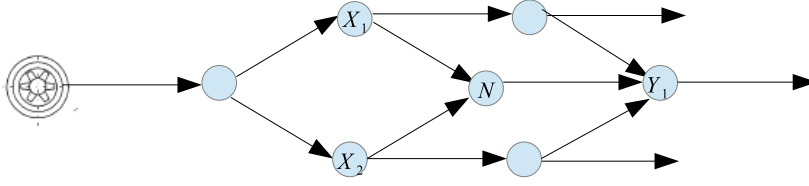


Fig. 2 Network Topology

$$\xi_1(x, t) = -\bar{\xi}_2 + \frac{\xi_1(0, t - \frac{x}{\lambda_1}) + \bar{\xi}_2}{\alpha \frac{x}{\lambda_1} (\xi_1(0, t - \frac{x}{\lambda_1}) + \bar{\xi}_2) + 1} \quad (36a)$$

Similarly, for the nonlinear approximation of the second wave, we obtain the following result:

$$\xi_2(x, t) = -\bar{\xi}_1 + \frac{\xi_2(L, t - \frac{(L-x)}{\lambda_2}) + \bar{\xi}_1}{\alpha \frac{(L-x)}{\lambda_2} (\xi_2(L, t - \frac{(L-x)}{\lambda_2}) + \bar{\xi}_1) + 1}. \quad (36b)$$

Taking into account the flow propagation of the waves described in Fig. 1 and equations (36a) and (36b) computed at the boundaries, we finally obtain the following delayed nonlinear equations:

$$\xi_1(L, t) = -\bar{\xi}_2 + \frac{\xi_1(0, t - h_1) + \bar{\xi}_2}{\alpha h_1 (\xi_1(0, t - h_1) + \bar{\xi}_2) + 1} \quad (37a)$$

$$\xi_2(0, t) = -\bar{\xi}_1 + \frac{\xi_2(L, t - h_2) + \bar{\xi}_1}{\alpha h_2 (\xi_2(L, t - h_2) + \bar{\xi}_1) + 1}. \quad (37b)$$

4 Network Model

The previous approximation of Euler's equations describes the flow transport in each pipe. The network model is obtained by considering a node as a finite control volume to which the pipes are connected. It is then possible to obtain a dynamical model for the fluid network, in terms of the transported variables. Fig. 2 shows a possible geometry of the networks studied in this work. Analyzing the dynamics of the transported variables in a specific node N of the network, the flow enters from the pipes connected to the nodes X_k and goes out to the pipes connected to the nodes Y_k . The propagation delay

$$h_1^{(X_k, N)} \quad (\text{respectively, } h_2^{(N, Y_k)})$$

is linked to the pipe length L and the characteristic velocity

$$\lambda_1^{(X_k, N)} \left(\text{respectively, } \lambda_2^{(N, Y_k)} \right).$$

4.1 Conservation at the Nodes and Fluid Capacitance

Taking into account the conservation for the physical variables ρ and q at a node N with n_{in} ingoing pipes and n_{out} outgoing pipe, the mass conservation at the intersection is stated as follows:

$$\sum_{i=1}^{n_{in}} q^{(X_i, N)}(L, t) = \sum_{i=1}^{n_{out}} q^{(N, Y_i)}(0, t), \quad \forall t > 0. \quad (38)$$

This condition is similar to Kirchhoff's law and is usually referred to as a Rankine-Hugoniot condition at the node [1, 2]. An additional coupling condition for the intersections is that the pressure inside each node is uniform (and thus the same at each extremity of the connected pipes), namely:

$$a^2 \rho^{(X_i, N)}(L, t) = a^2 \rho^{(N, Y_k)}(0, t) = \text{constant} \quad \forall i = 1, \dots, n_{in}, \forall k = 1, \dots, n_{out} \quad (39)$$

With the transformations (7) and (8), we can use (39) to state that $\forall i = 1, \dots, n_{in}$ and $\forall k = 1, \dots, n_{out}$, we have:

$$\xi_1^{(X_i, N)}(L, t) - \xi_2^{(X_i, N)}(L, t) = \xi_1^{(N, Y_k)}(0, t) - \xi_2^{(N, Y_k)}(0, t) = \text{constant}, \quad (40)$$

The constraint (38) implies that

$$\sum_{i=1}^{n_{in}} \xi_1^{(X_i, N)}(L, t) + \xi_2^{(X_i, N)}(L, t) = \sum_{k=1}^{n_{out}} \xi_1^{(N, Y_k)}(0, t) + \xi_2^{(N, Y_k)}(0, t). \quad (41)$$

A dynamics is introduced to model the fluid capacitance as a time-varying state associated with the node. Denoting the fluid capacitance as C_f , it follows that at node N :

$$\dot{P}(t)^N = q^N / C_f \quad (42)$$

$$\Leftrightarrow \dot{P}(t)^N = -\frac{M_g}{ZRTC_f} q^N = -\frac{M_g}{ZRTC_f} \left(\sum_{i=1}^{n_{in}} \xi_1^{(X_i, N)}(L, t) + \xi_2^{(X_i, N)}(L, t) - \sum_{k=1}^{n_{out}} \xi_1^{(N, Y_k)}(0, t) + \xi_2^{(N, Y_k)}(0, t) \right) \rho^N \quad (43)$$

where we used (1) with the isothermal hypothesis, (7), (8) and (41). Note that C_f could also be node-dependent to capture large changes in the network configuration. It is then possible to represent the node with an equivalent Bond graph description composed of a 0-junction (using constant effort and the fact that the sum of the

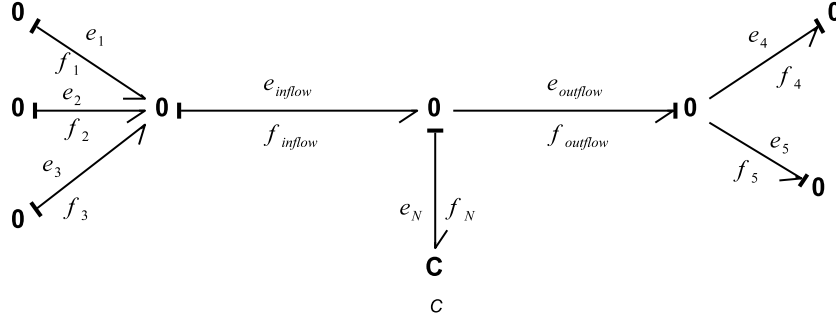


Fig. 3 Expanded Bond Graph Representation of the Node

inflows is equal to the sum of the outflows) and a C-element. Fig. 3 shows the equivalent Bond graph representation for a node. The constraints (40) and (43) are then satisfied if we define the effort as $e = \xi_1 - \xi_2$ and the flow as $f = \xi_1 + \xi_2$ for each junction.

Choosing the internal state of the node as e^N and expressing (43) in terms of e^N using (7)-(8), we have that:

$$e^N = -\alpha_c \left(\sum_{i=1}^{n_{in}} \xi_1^{(X_i, N)}(L, t) + \xi_2^{(X_i, N)}(L, t) - \sum_{k=1}^{n_{out}} \xi_1^{(N, Y_k)}(0, t) + \xi_2^{(N, Y_k)}(0, t) \right) \quad (44)$$

$$\xi_1^{(X_i, N)}(L, t) - \xi_2^{(X_i, N)}(L, t) = \xi_1^{(N, Y_k)}(0, t) - \xi_2^{(N, Y_k)}(0, t) = e^N \quad (45)$$

where $\alpha_c = aM_g/ZRTC_f$. The node is thus well defined by an algebro-differential system of equations and the corresponding Riemann invariants are computed in each branch by adding or subtracting the effort and flow. Note that the flow inertia and friction are already taken into account within the Euler equations with friction.

4.2 State-Space Representation

The previous bond-graph description can be expressed as a classical state-space representation, as follows. Considering that ξ_1 enters the node from the left and that ξ_2 enters the node from the right, we wish to establish a mapping between the inputs $\{\xi_1^{(X, N)}(L, t), \xi_2^{(N, Y)}(0, t)\}$ and the outputs $\{\xi_1^{(N, Y)}(0, t), \xi_2^{(X, N)}(L, t)\}$, where we used the notation X and Y (without subscripts) to denote the column vectors containing all the inflow or outflow components, respectively. The effort relationships (40) and (45) imply that:

$$\begin{aligned} & \begin{bmatrix} \xi_1^{(X,N)}(L,t) \\ \xi_1^{(N,Y)}(0,t) \end{bmatrix} - \begin{bmatrix} \xi_2^{(X,N)}(L,t) \\ \xi_2^{(N,Y)}(0,t) \end{bmatrix} = \mathbf{1}^{(n_{in}+n_{out}) \times 1} e^N \\ \Leftrightarrow & \begin{bmatrix} \xi_2^{(X,N)}(L,t) \\ -\xi_1^{(N,Y)}(0,t) \end{bmatrix} = -\mathbf{1}^{(n_{in}+n_{out}) \times 1} e^N + \begin{bmatrix} \xi_1^{(X,N)}(L,t) \\ -\xi_2^{(N,Y)}(0,t) \end{bmatrix} \end{aligned} \quad (46)$$

where $\mathbf{1}^{i \times j}$ is a vector of ones of size $i \times j$. Considering (44), the node dynamics is then:

$$\begin{aligned} \dot{e}(t)^N &= -\alpha_c \left(\begin{bmatrix} \mathbf{1}^{1 \times n_{in}} & \mathbf{1}^{1 \times n_{out}} \end{bmatrix} \begin{bmatrix} \xi_1^{(X,N)}(L,t) \\ -\xi_2^{(N,Y)}(0,t) \end{bmatrix} + \begin{bmatrix} \mathbf{1}^{1 \times n_{in}} & \mathbf{1}^{1 \times n_{out}} \end{bmatrix} \begin{bmatrix} \xi_2^{(X,N)}(L,t) \\ -\xi_1^{(N,Y)}(0,t) \end{bmatrix} \right) \\ &= -\alpha_c e^N - 2\alpha_c \begin{bmatrix} \mathbf{1}^{1 \times n_{in}} & \mathbf{1}^{1 \times n_{out}} \end{bmatrix} \begin{bmatrix} \xi_1^{(X,N)}(L,t) \\ -\xi_2^{(N,Y)}(0,t) \end{bmatrix} \end{aligned} \quad (47)$$

We thus obtained a state-space description where (47) describes the state dynamics and (46) determines the output

$$\begin{bmatrix} \xi_2^{(X,N)}(L,t) \\ -\xi_1^{(N,Y)}(0,t) \end{bmatrix}$$

from the input (direct feedthrough)

$$\begin{bmatrix} \xi_1^{(X,N)}(L,t) \\ -\xi_2^{(N,Y)}(0,t) \end{bmatrix}$$

and the state e^N .

4.3 Interconnections and Delays

We can now consider the interconnections on node N with its predecessors X and successors Y . The linear approximation of the pipe propagation waves and the delayed equations (28a) and (28b) along with the previous node description imply that:

$$\dot{e}(t)^N = -\alpha_c e^N - 2\alpha_c \begin{bmatrix} \mathbf{1}^{1 \times n_{in}} & \mathbf{1}^{1 \times n_{out}} \end{bmatrix} u(t) \quad (48)$$

$$\begin{bmatrix} \xi_2^{(X,N)}(L,t) \\ -\xi_1^{(N,Y)}(0,t) \end{bmatrix} = -\mathbf{1}^{(n_{in}+n_{out}) \times 1} e^N + u(t) \quad (49)$$

with

$$u(t) = \begin{bmatrix} \xi_1^{(X,N)} \left(0, t - h_1^{(X,N)} \right) e^{2\alpha(\bar{\xi}_1^{(X,N)} + \bar{\xi}_2^{(X,N)})h_1^{(X,N)}} \\ -\xi_2^{(N,Y)} \left(L, t - h_2^{(N,Y)} \right) e^{2\alpha(\bar{\xi}_1^{(N,Y)} + \bar{\xi}_2^{(N,Y)})h_2^{(N,Y)}} \end{bmatrix} \quad (50)$$

Each node is thus defined by a delay differential equation with a direct feedthrough of the interconnection variable $u(t)$ on the output. This interconnection variable is obtained from the outputs of the predecessors (terms in $\xi_1^{(X,N)}$) and of the successors (terms in $\xi_2^{(N,Y)}$).

The nonlinear approximation is obtained in a similar way by taking into account the functional equations (37a) and (37b). The delayed differential equation is then given by (48)-(49) with the interconnection:

$$u(t) = \begin{bmatrix} -\bar{\xi}_2^{(X,N)} + \frac{\xi_1^{(X,N)}(0, t - h_1^{(X,N)}) + \bar{\xi}_2^{(X,N)}}{\alpha h_1^{(X,N)} \left(\bar{\xi}_1^{(X,N)}(0, t - h_1^{(X,N)}) + \bar{\xi}_2^{(X,N)} \right) + 1} \\ \bar{\xi}_1^{(N,Y)} - \frac{\xi_2^{(N,Y)}(L, t - h_2^{(N,Y)}) + \bar{\xi}_1^{(N,Y)}}{\alpha h_2^{(N,Y)} \left(\bar{\xi}_2^{(N,Y)}(L, t - h_2^{(N,Y)}) + \bar{\xi}_1^{(N,Y)} \right) + 1} \end{bmatrix} \quad (51)$$

5 Simulations Results

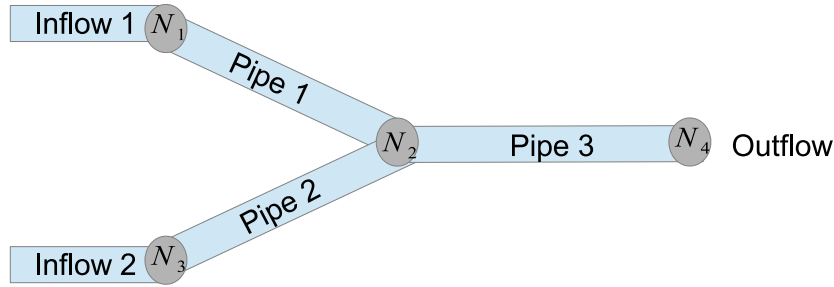
Consider the network configuration shown in Fig. 4, corresponding to an air ventilation network, where the speed of sound constant is $a = 347m/s$. The network parameters are given in Table 1. The inflow (i.e. boundary conditions) is considered as con-

Parameter	Pipe 1	Pipe 2	Pipe 3
Length (L)	100m	200m	300m
Diameter (D)	0.4m	0.2m	0.4m
Friction factor (f_g)	0.008	0.0012	0.003

Table 1 Pipe Parameters of the Network

stant and the initial conditions are $\rho(t, 0) = 1.16 kg/m^3$ and $q(t, 0) = 23.2 kg/m^2 s$. We perform numerical simulations of the network model derived in the previous sections and compare the linear and nonlinear delay differential equations in Fig. 5. The results are presented for each node of the network in terms of the physical variables, density and momentum, which can be found directly from the Riemann invariants by using the transformation (7) and (8), respectively. According to the network parameters, the time delays and friction terms are presented in Table 2.

We can clearly observe the propagation delays on these simulation, as well as the oscillations due to wave reflections and coupling at the nodes. It is also interesting to note the closeness between the linear and the nonlinear models, which suggests that linear control approaches may provide satisfactory results despite the nonlinear characteristic of the friction phenomenon.

**Fig. 4** Network Example

Parameter	Value	Parameter	Value	Parameter	Value	Parameter	Value
$h_1^{(1)}$	0.2725	$h_2^{(1)}$	0.3058	$\beta^{(1)}$	0.9470	$\beta^{(5)}$	0.9407
$h_1^{(2)}$	0.5450	$h_2^{(2)}$	0.6116	$\beta^{(2)}$	0.9678	$\beta^{(6)}$	0.9640
$h_1^{(3)}$	0.8174	$h_2^{(3)}$	0.9174	$\beta^{(3)}$	0.9521	$\beta^{(7)}$	0.9464
$h_1^{(4)}$	0.1362	$h_2^{(4)}$	0.1529	$\beta^{(4)}$	0.9967	$\beta^{(8)}$	0.9963

Table 2 Simulation Network Parameters

6 Conclusion

A time-delay approach is used in this work to find a model for the flow in fluid networks. The model of the flow is taken from the isothermal Euler equations. The hyperbolic characteristics of the PDE system are taken into account in order to diagonalize the system. The method of characteristics is considered to find functional equations related to the isothermal Euler equations. By decoupling the incoming and outgoing waves and averaging the source term on the appropriate components, two approximations are adopted to compute a delayed model of the flow, namely a linear approximation and a nonlinear one. Taking into account the conservative characteristics at the nodes, a delay differential system of equations for the flow network is finally given.

References

1. Banda, M., Herty, M., Klar, A.: Coupling conditions for gas networks governed by the isothermal Euler equations. *Networks and Heterogeneous Media* 1(2), 295–314 (2006)
2. Banda, M., Herty, M., Klar, A.: Gas flow in pipeline networks. *Networks and Heterogeneous Media* 1(1), 41–56 (2006)
3. Bradu, B., Gayet, P., Niculescu, S-I., Witrant, E.: Modeling of the very low pressure helium flow in the LHC cryogenic distribution line after a quench. *Cryogenics* 50(2), 71–77 (2010)
4. Bresch-Pietri, D., Leroy, T., Petit, N.: Control-oriented time-varying input-delayed temperature model for SI engine exhaust catalyst. In: *Proceedings of the American Control Conference*, pp. 2189–2195 (2013)

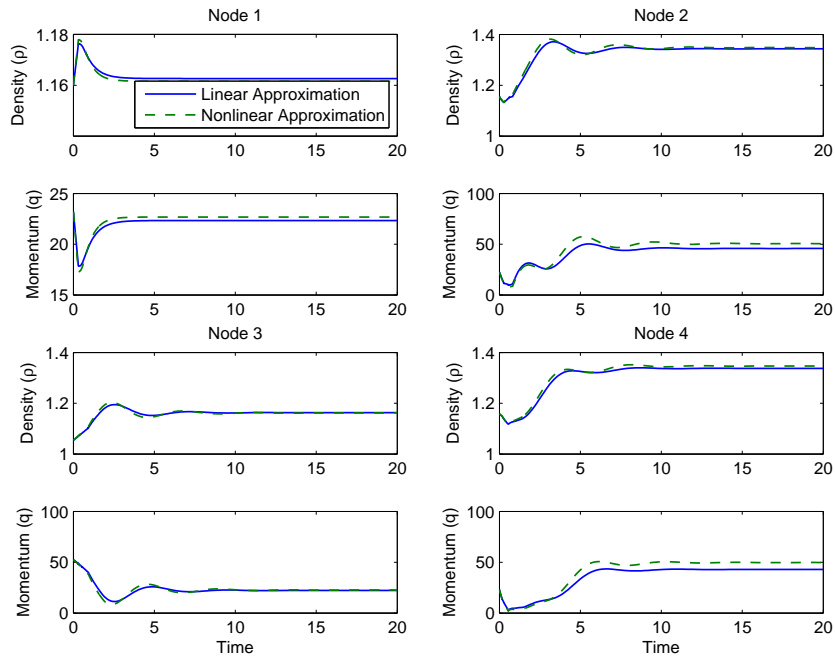


Fig. 5 Dynamics of the Physical Variables in the Network Nodes

5. Colombo, R., Guerra, G., Herty, M., Schleper, V.: Optimal control in networks of pipes and canals. *SIAM Journal on Control and Optimization* 48(3), 2032–2050 (2009)
6. Cooke, K., Krumme, D.: Differential-difference equations and non-linear partial-boundary value problems for linear hyperbolic partial differential equations. *Journal of Mathematical Analysis and Applications* 24(2), 362–387 (1968)
7. Corrigan, G., Sanna, S., Usai, G.: Sub-optimal constant-volume control for open channel networks. *Applied Mathematical Modelling* 7(4), 262 – 267 (1983)
8. Cross, H.: Analysis of flow in networks of conduits or conductors. University of Illinois Engineering Experiment Station Bulletin 286 (1936)
9. de Halleux, J., Prieur, C., Coron, J-M., d’Andrea Novel, B., Bastin, G.: Boundary feedback control in networks of open channels. *Automatica* 39(8), 1365–1376 (2003)
10. de Saint-Venant, B.: Theorie du mouvement non-permanent des eaux avec applications aux crues des rivieres et a l’introduction des mares dans leur lit. *Comptes-rendus de l’Academie des Sciences* 73, 148–154 (1871)
11. Dick, M., Gugat, M., Herty, M., Steffensen, S.: On the relaxation approximation of boundary control of the isothermal Euler equations. *International Journal of Control* 8(11), 1766–1778 (2012)
12. Evans, L.: *Partial Differential Equations*. Series Graduate Studies in Mathematics Volume 19. American Mathematical Society, Providence, RI (1998)
13. Gugat, M., Herty, M., Schleper, V.: Flow control in gas networks: Exact controllability to a given demand. *Mathematical Methods in the Applied Sciences* 34(7), 745–757 (2011)
14. Gugat, M., Dick, M.: Time-delayed boundary feedback stabilization of the isothermal Euler equations with friction. *Mathematical Control and Related Fields* 1(4), 469–491 (2011)
15. Hartman, H., Mutmanský, J., Ramani, R., Wang, Y.: *Mine Ventilation and Air Conditioning*, Third Edition. Wiley, New York (1997)

16. Hirsch, C.: Numerical Computation of Internal and External Flows: The Fundamentals of Computational Fluid Dynamics, Second Edition. Elsevier, New York (2007)
17. Hu, Y., Koroleva, O., Krstic, M.: Nonlinear control of mine ventilation networks. *Systems and Control Letters* 49(4), 239-254 (2003)
18. Karafyllis, I., Krstic, M.: On the relation of delay equations to first-order hyperbolic partial differential equations. *ESAIM Control, Optimisation and Calculus of Variations* 20(3), 894–923 (2014)
19. Koroleva, O., Krstic, M.: Averaging analysis of periodically forced fluid networks. *Automatica* 41(1), 129-135 (2005)
20. Litrico, X., Georges, D.: Robust continuous-time and discrete-time flow control of a dam-river system. *Applied Mathematical Modelling* 23(11), 809–827 (1999)
21. Litrico, X., Fromion, V.: Analytical approximation of open-channel flow for controller design. *Applied Mathematical Modelling* 28(7), 677–695 (2004)
22. Petrov, N., Shishkin, M., Dmitriev, V., Shadrin, V.: Modeling mine aerology problems. *Journal of Mining Science* 28(2), 185–191 (1992)
23. Rasvan, V.: Functional differential equations and one-dimensional distortionless propagation. *Tatra Mountains Mathematical Publications* 43(1), 215–228 (2009)
24. Rasvan, V.: Delays. Propagation. Conservation Laws. In: Sipahi, R., Vyhlidal, T., Niculescu, S-I., Pepe, P. (eds.) *Time delay systems: Methods, Applications and New Trends. Series Lecture Notes in Control and Information Sciences Volume 423*, pp. 147–159. Springer, New York (2012)
25. Rasvan, V.: Three lectures on neutral functional differential equations. *Journal of Control Engineering and Applied Informatics*. 11(9), 49-55 (2009)
26. Toro, E.: *Riemann Solvers and Numerical Methods for Fluid Dynamics*, Third Edition. Springer, New York (2009)
27. Treiber, M., Kesting, A.: *Traffic Flow Dynamics: Data, Models and Simulation*. Springer, Berlin Heidelberg (2013)
28. Witrant, E., Johansson, K.: Air flow modeling in deepwells: Application to mining ventilation. In: *Proceedings of the IEEE International Conference on Automation Science and Engineering*, pp. 845–850 (2008)
29. Witrant, E., Marchand, N.: Modeling and feedback control for air flow regulation in deep pits. In Sivasundaram, S. (ed.) *Mathematical Problems in Engineering, Aerospace and Sciences*. Cambridge Scientific Publishers, Cambridge, UK (2011)
30. Witrant, E., Niculescu, S-I.: Modeling and control of large convective flows with time-delays. *Mathematics in Engineering, Science and Aerospace* 1(2), 191–205 (2010)